Arch. Metall. Mater. **69** (2024), 4, 1491-1499

DOI: https://doi.org/10.24425/amm.2024.151419

N.A. NASRUN[1], N.F.M. YUNOS[2,3*], M.A. IDRIS[1,3], N.A. HALIF[1,3], T. NOMURA[4]

THE EFFECT OF PALM CHAR PROPERTIES ON MALAYSIAN ILMENITE ORES BY CARBOTHERMAL REDUCTION

To identify the mineral grade ore, two distinct Malaysian ilmenite ores ($FeTiO_3$) from different placers deposits were examined. The sources of ilmenite ore were the Kinta Valley in Perak and the Langkawi Black Sand Beach in Kedah. Both of the ores were reduced by palm char as a sustainable carbon reductant. The study examined carbon characteristics and phase transitions following carbothermal reduction at 1550°C. Prior to the studies, the reductant palm char was characterized by XRF, BET surface area measurement, SEM, and ultimate with proximate analyses. It is shown that the palm char had low moisture (4.10 wt.%) and high fixed carbon (75.40 wt.%). The high carbon content, volatile matter, and porous structure of palm char played a significant role in the gas generated during the carbothermal reduction of ilmenite ores. Carbothermal reduction of both ilmenite ores with palm char-produced rutile, iron, titanium carbide, and pseudobrookite. The XRF analysis exhibits the existence of 18.41 and 35.76 wt.% of Fe and TiO_2 respectively in Perak ilmenite ore. While Langkawi ilmenite ore shows 9.28 and 22.72 wt.% of Fe and TiO_2 respectively.

Keywords: Malaysian ilmenite ores; Palm char; Carbothermal reduction; Titanium dioxide

1. Introduction

In Malaysia, the main resources of ilmenite were from Perak, Selangor, Pahang, and Kedah. The deposit placer of ilmenite ore in Malaysia indicated that the percent of TiO_2 in ilmenite was found in Langkawi (29.7 wt.%) lower than in Selangor (52.48 wt.%) and Perak (54.31 wt.%) [1-3]. Ilmenite ($FeTiO_3$) and pseudobrookite (Fe_2TiO_5) phases were found in Perak ilmenite due to mild weathering and alteration processes [4] while Langkawi ilmenite ore mostly consisted of $FeTiO_3$ and titanomagnetite (Fe_2TiO_4-Fe_3O_4) phases with considerable impurities such as quartz [5].

It is well known that high-quality ilmenite ore was highly attractive in the mineral processing industry since it can be directly converted into rutile, TiO_2 pigments, and titanium metal. However, low and medium-quality of ilmenite ore required an expensive process to convert into titanium slag or synthetic rutile [6,7]. Ilmenite ore had different properties and chemical compositions at distinct placer deposits [8] and was graded by the percentage of TiO_2 and Fe_2O_3 content. A low grade of ilmenite ore was considered in the range of <28 wt.% of TiO_2 while high-grade ore was above 55 wt.% [8,9]. Ilmenite containing high TiO_2 would present as rutile and psuedorutile. On the other hand, aluminosilicates in ilmenite ore were considered medium and low-grade ore while a high-grade ore of ilmenite is considered to have high TiO_2 with a low amount of Fe_2O_3 [10]. Ilmenite ore from the alteration process was mainly contained of psuedorutile phase.

Ilmenite ore can be upgraded into synthetic rutile by using two methods; (i) ilmenite ore reduced with separation by acid leaching and (ii) ilmenite ore reduction (carbothermal) and aeration [11]. The carbothermal reduction process of ilmenite ore used carbon sources from coal and graphite. However, due to the high amount of sulfur, nitrogen, and ash in coal, this process caused environmental problems [3]. On the other hand, graphite was more expensive carbon reductants compared to another carbon sources for carbothermal reduction process [12,13]. The high cost of the production of coal and graphite led the titanium industry to seek other alternating or renewable carbon reductants from agricultural waste such as coconut shells, wood powder, and sawdust as carbon reductants [14,15]. Thus, the present study proposed to used palm char as an alternative carbon resource since the fixed carbon was almost similar to coal/coke properties [16,17]. The palm char contained a porous structure with a high

[1] UNIVERSITI MALAYSIA PERLIS (UNIMAP), FACULTY OF CHEMICAL ENGINEERING & TECHNOLOGY, 02600 ARAU PERLIS, MALAYSIA
[2] UNIVERSITI MALAYSIA PERLIS (UNIMAP), FACULTY OF MECHANICAL ENGINEERING & TECHNOLOGY, 02600 ARAU PERLIS, MALAYSIA
[3] UNIVERSITI MALAYSIA PERLIS (UNIMAP), FRONTIER MATERIALS RESEARCH, CENTRE OF EXCELLENCE (FRONTMATE), MALAYSIA
[4] HOKKAIDO UNIVERSITY, CENTRE FOR ADVANCED RESEARCH OF ENERGY AND MATERIALS, KITA 13 NISHI 8 KITA-KU SAPPORO 060-8628, JAPAN

* Corresponding author: farhanadiyana@unimap.edu.my

surface area and graphitic structure were found to increase the carbothermal reduction reactions [17-19].

The common methods of converting ilmenite ore into TiO_2 or Ti phase was through smelting in an electric arc furnace and making high titania slag, the hydrometallurgical process, or the solid-state extraction FFC Cambridge process [20]. However, all these processes required high-energy consumables with the problem of oxidation and are non-environmentally friendly since using toxic products. Thus, using carbothermal reduction for ilmenite reduction is beneficial and also environmental since palm char is a renewable carbon reductant that could reduce carbon dioxide (CO_2) emissions [16]. There are two primary phases ($Fe_{(m)}$ and pseudobrookite) generated in carbothermal reduction utilising palm char as a carbon reductant. According to Setiawan et al., pseudobrookite was found to be a minor phase due to its low quantity or sluggish production kinetics, whereas pseudobrookite was found in samples reduced at 1100°C and 1200°C [15]. Mohammed et. al investigated the carbothermal reduction of ilmenite ore with palm char at 1400°C. The ilmenite ore reduced the $FeTiO_3$ phase by palm char into TiC, iron titania, and titanium suboxides including TiO_2 phases [18]. From the literature, most of the research only focuses on carbon sources from graphite, coke/coal, and activated carbon at low carbothermal reduction temperatures (1000-1400°C) [2,19,21]. However, there is limited study on the understanding of the carbon reductant characteristics, especially from palm char in carbothermal reduction at a high-temperature reaction of 1550°C. In addition, two types of Malaysian ilmenite ore will be investigated the possible mineral ore deposit placer in Malaysia for exploration and to determine the ore grades for upgrading the local mineral processing using this carbothermal reduction method.

2. Experimental

2.1. Materials & sample preparations

The ilmenite ore was collected from two locations: one from Langkawi's Black Sand Beach in Kedah (medium-grade ore), and the other from Kinta Valley in Perak (high-grade ore). Ilmenite ores were dried, and then magnetic separation was used to extract the ilmenite ore from the placer deposit (sands or soil) using a magnetic field of 6000-6500 gauss. After separation, only the magnetic materials from the separation are used and sieved into a fine particle size of 63 μm after the milling process.

The as-received palm shell was dried for 24 hours in an oven to remove its moisture. The palm shell is fragmented into small pieces after drying to became around 2 mm in size. The fast pyrolysis technique was then applied to convert the palm shells into palm char in a horizontal tube furnace with an end-closed tube, the heating rate was fixed to 10°C/min at 450°C for two hours in nitrogen gas. The flow rate of the nitrogen gas was set to 0.5 L/min.

Then ilmenite ore was mixed with palm char using a molar ratio of 1:3, calculated from the total carbon reducible with oxygen in ilmenite. The mixed samples were pelletized in a die mold of 10 mm in diameter.

2.2. Carbothermal reduction reaction

A horizontal tube furnace was used to carry out the carbothermal reduction procedure, which took place at 1550°C for 20 minutes of reaction. The heating profile is specified to have an inert argon gas flow rate of 0.5 L/min and a heating rate of 10°C/min. At desired temperature, the sample was put in an alumina crucible in the cold zone before being pushed inside the tube furnace for 5 minutes to prevent an oxidation reaction. The samples were then slowly inserted into the hot area of the furnace. The gas generations (CO and CO_2) were monitored using gas analyser continuously during carbothermal reduction process. The furnace setup has already been published elsewhere [18,22].

2.3. Characterizations

The chemical compositions of palm shells, palm char, and ilmenite ores were examined using X-ray fluorescence (PANalytical Minipal4).The proximate analysis of carbon reductants was used to investigate the total moisture (ASTM D3173), ash content (ASTM D7582-12), and volatile (ASTM D2974). The ultimate analysis CHNS analyzer (Perkin Elmer 2400 Series II) was used to determine carbon, hydrogen, sulfur, and nitrogen content in palm shells and palm char.

The phase transformations analysis was performed using X-Ray Diffraction (XRD) (Bruker D2) with CuKα radiation that operated at 30 kV and 30 mA with the scanning rate at 2° in ranges of 10°-80° with a step size of 0.02°. The peak analysis was based on the Inorganic Crystal Structure Database (ICSD) referred to as Powder Diffraction File (PDF). The surface morphology determines the changes in structure and porous material by Scanning Electron Microscope (SEM). The operating parameter for surface morphology was set voltage 10 kV using secondary electron (SE). BET surface area measurements were conducted to determine the pore surface area with adsorption and desorption analysis. The carbon reductants were prepared with a size of 90 μm with a weight of 500 mg. Then, the samples were degassed for 2 hours using nitrogen gas at a temperature of 300°C. In addition, the thermodynamics calculation and reaction on free Gibbs Energy was calculated by HSC Chemistry software [18].

3. Results & discussion

3.1. Malaysian ilmenite ores characterizations

3.1.1. Chemical composition analysis

The chemical composition of two Malaysian ilmenite ores from Perak and Langkawi was determined using XRF presented

TABLE 1

Chemical composition (wt.%) of different grades of Malaysian ilmenite ore using XRF analysis

Deposit Placer	TiO_2	Fe_2O_3	Na_2O	MgO	Al_2O_3	SiO_2	P_2O_5	SO_3	K_2O	CaO
Perak	71.27	18.85	0.39	0.64	n.d	2.72	0.13	0.03	0.12	0.10
Langkawi	34.24	16.25	0.52	0.38	23.92	22.32	—	0.03	0.23	0.53

in TABLE 1. The major element was titanium dioxide (TiO_2) and hematite (Fe_2O_3) in both ilmenite deposit placers, however, Langkawi ilmenite contained high silica (SiO_2) and alumina (Al_2O_3) compared to Perak ilmenite. This was due to the location of the deposit placer where Langkawi black sand beach is surrounded by silica sands. Furthermore, high silica is also anticipated from the magnetic separation procedure [5,23]. These oxide phases are also detected in the XRD analysis (Fig. 1(b)). TiO_2 from Perak ilmenite (71.27 wt%) was greater than in Langkawi ilmenite (34.24 wt.%), according to TABLE 1. The findings supported the classification of Perak ilmenite as a high-grade ore and Langkawi ilmenite as a medium-grade ore [9,24].

3.1.2. Phase Analysis

The phase analysis of untreated Perak ilmenite is shown in Fig. 1(a). According to the figure, Perak ilmenite was composed of the phases hematite (Fe_2O_3), ilmenite ($FeTiO_3$), rutile (TiO_2) ICSD# 03-065-0192, brookite (TiO_2) ICSD# 00-021-1276, and anatase (TiO_2) ICSD# 98-000-9852. The $FeTiO_3$ identified by the ICSD# 96-900-0908, space group R-3, and space group number 148 in a hexagonal crystal system. $FeTiO_3$ phases existed at angles 32.41°, 35.11°, 40.13°, 48.13°, 48.52°, 52.84°, 56.02°, 61.29°, 62.99° and 69.83°. Hematite phase detected at angle of $2\theta = 24.30°$ with crystal plane (0 1 2) referred to ICSD# 96-591-0083 with hexagonal crystal system while silicon dioxide detected at 27.33° with crystal plane (1 0 1). From the figure, TiO_2 (Anatase) located at angle of 25.69° with crystal plane (0 1 1), meanwhile TiO_2 (Rutile) phases appeared at $2\theta = 27.43°$, 41.24°, 54.32° and 27.43° with crystal plane (1 1 0). The brookite phase existed at an angle of 25.69°, where pure brookite samples can be a mixture of anatase and brookite. Based on the chemical composition discovered in the Perak ilmenite, which has a high weight percentage of 71.27 wt.% (TABLE 1), XRD analysis was able to detect the maximum proportion of TiO_2 phases, confirming the high-grade grade quality of this ore. Ahmadi et al. investigated the grade of Malaysian ilmenite and discovered the primary phases were pseudobrookite and ilmenite. The weathering process may have caused the pseudobrookite phase to exist [25].

Fig. 1(b) represents raw Langkawi ilmenite contained phases of titanomagnetite ($Fe_{2.75}Ti_{0.25}O_4$), magnetite (Fe_3O_4), silicon dioxide (SiO_2), hematite (Fe_3O_4), TiO_2 (rutile, anatase, and brookite). The titanomagnetite was detected at angles $2\theta = 15°$ and 35.41° with a crystal plane (1 1 3). Magnetite phase existed at angles $2\theta = 18.54°$, 30.58° and 63.653° while hematite phases at angles of 57.57°, 62.40° and 88.50°. The main phase in Langkawi ilmenite ore was phase detected at 23.71°, 32.52°, 34.988°, 48.510°, 52.983°, 61.20°, and 73.913°. Silicon dioxide (quartz) also existed at angles of 21.197°, 27.028°, 42.489°, 45.83° and 60°. This quartz was high in Langkawi ilmenite compared to Perak ilmenite (TABLE 1) due to the distinct deposit placer [5,16,26]. Based on the X-ray diffraction patterns of 2 different Malaysian ilmenite ores, it was predicted that the carbothermal reduction process converted the the anatase and brookite phases into the rutile phase. It signifies that TiO_2's anatase phase is unstable at temperatures higher than 800°C [27]. Brookite and anatase phases were found between 500 and 600°C while rutile phase was seen stable at 800°C. The amount of rutile increased significantly [21].

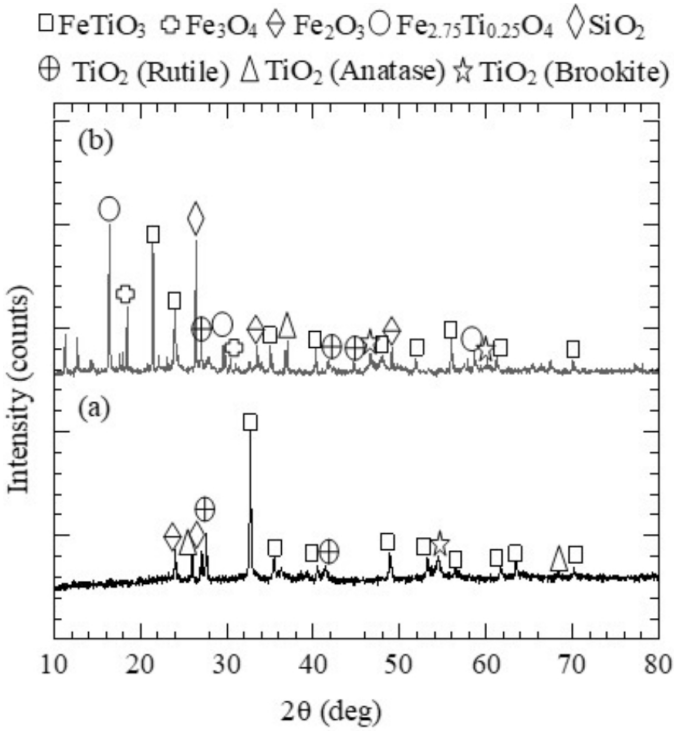

Fig. 1. Phase analysis of Malaysian ilmenite ores using XRD (a) Perak ilmenite and (b) Langkawi ilmenite

3.2. Carbon reductant characterizations

3.2.1. Chemical composition analysis

According to TABLE 2, the raw palm shells comprised 40.30 wt.% carbon, 2.59 wt.% of hydrogen, 56.44 wt.% of oxygen, 0.4545 wt.% of nitrogen and 0.22 wt.% of sulphur. The proximate composition of palm shell was 6.60% of moisture matter, 17.30% volatile matter, 24.30% ash matter and

TABLE 2

Proximate analysis and elemental composition of palm shell and palm char

Samples	Proximate analysis (wt.%)				Elemental composition (wt.%)				
	Moisture	Volatile matter	Ash	Fixed Carbon	C	H	O	N	S
Palm shell	6.60	17.30	24.30	42.40	40.30	2.59	56.44	0.45	0.22
Palm char	4.10	10.90	15.00	75.40	75.72	3.18	20.11	0.81	0.18

42.40 wt.% of fixed carbon. The palm shell is used as a fuel in the production of iron and the extraction of minerals due to its reduced sulphur content, which varies from 0.5 to 0.8 wt.%. High sulphur concentration in coal and coke was shown to slow down the carbothermic reduction reaction rates [28,29]. To produce a high-quality metal throughout the iron-making and metal extraction processes, the sulphur level in the carbon reductant must be between 0.5 and 0.8 wt.% and low moisture below 7.0 wt.% [30,31]. The current results indicated that palm char had less sulfur and low moisture content. The production of iron and the extraction of metals demonstrated that agricultural wastes or biomass are mostly composed of higher levels of C, H, and O and lower levels of N and S than pulverised coal or coke [5]. Agricultural waste also contained less N and S, which results in reduced NO_x and SO_x emissions from burning or reduction [32,33]. The current results indicated that palm char had less sulfur and low moisture content.

After pyrolysis, the palm char had a moisture content of 4.10 wt.%, a volatile content of 10.90 wt.%, an ash content of 15.0 wt.%, with fixed carbon content of 75.40 wt.% (TABLE 3). The ash content dropped from 24.30 to 15 wt.%. Lower ash encouraged the reactivity of metal oxide, which is advantageous for the carbothermal reduction of ilmenite [32]. Low ash concentration also eliminates sludging and agglomeration issues in horizontal tube furnaces during carbothermal reduction [34,35]. The amount of fixed carbon in palm char increased from 42.50 to 75.40 wt.% while the amount of volatile matter fell from 17.30 to 10.90 wt.%. The increase in carbon content in the palm char was influenced by the pyrolysis temperature and devolatilization stage [36].

The carbon content increased at high temperature (450°C) due to the fast pyrolysis process. This process was involved in breaking the bonding between hydrogen, nitrogen and oxygen present in the palm char structure due to weaker bonds from carboxyl and hydroxyl groups [37]. The product of palm char developed the desirable properties of rich-carbon content, low volatile and oxygen, that classified as high resistance to chemical reaction from hydrolysis or oxidation process [36]. Since palm char has >70 wt.% of carbon that is similar to coke's characteristics and contributes to a high reduction product yield, it can be utilised as a carbon reductant [30,38].

The chemical composition of raw palm shells and palm char are listed in TABLE 3. Both samples contained organic materials (alkali metal in the form of oxides) in their ash. Raw palm shells had a higher percentage of ash (24.3 wt.%) than palm char (15 wt.%), according to TABLE 2. The type of soil where the palm tree which produced the palm kernel shells was nurtured was the cause of the high concentration of SiO_2 (22.77 wt.%) and Fe_2O_3 (57.997 wt.%) in the ash of raw palm shells. The soils with fertilizer are also affected due to the high oxide compounds in the raw palm shells [39]. After palm shells were converted into palm char, it was found that the palm char contained inorganic matter in form of oxides with 35.93 wt.% of Fe_2O_3 and also 37.90 wt.% of SiO_2 (TABLE 3). It is expected that the inorganic materials had an influence on the formation of gas, tar, and char from woody biomass (>800°C) [40]. The generation of gas and hydrocarbons released during pyrolysis contributed to raising the rates of carbothermal and iron reduction, respectively [1,18]. Another crucial indicator of a carbon reductant's reactivity is the composition of the ash content [41]. Furthermore, it is known that the sodium and potassium oxides act as catalysts in gas phase processes [42]. The easy-to-vaporize alkali metals in palm char improved the reduction rate by expediting the gas diffusion. [43].

3.2.2. Porous characteristics and microstructure analysis

The palm shell and palm char SEM micrographs were seen as in Fig. 2(a) and 2(b). Before the thermal conditions, the cell structure of palm char was hexagonal. Small pores are scattered across the surface of the raw palm shell, which appears to be defined by ordered compact cells. It is expected that the structure of the shells will alter noticeably during pyrolysis. Micrographs of the char's exterior surfaces taken at 450°C (Fig. 2(b)) revealed that the wall rupture and eventual destruction of the hexagonal structure's cell lumen. The removal of cell walls caused by volatile matter evaporation led to the opening of pore structures, which in turn has resulted in porous networks [44]. The results are consistent with the volatile matter content dropping from 17.30 to 10.90 wt.% as shown in TABLE 2, and the BET surface

TABLE 3

Elemental compositions (wt.%) of palm shell and palm char

Elements	Na_2O_3	MgO	Al_2O_3	SiO_2	P_2O	SO_2	K_2O_3	CaO	TiO_2	Fe_2O_3
Palm shell	1.55	1.60	9.36	22.77	0.16	0.18	3.45	1.74	0.73	57.99
Palm char	1.02	—	10.83	37.90	0.24	0.13	7.04	3.87	2.46	35.92

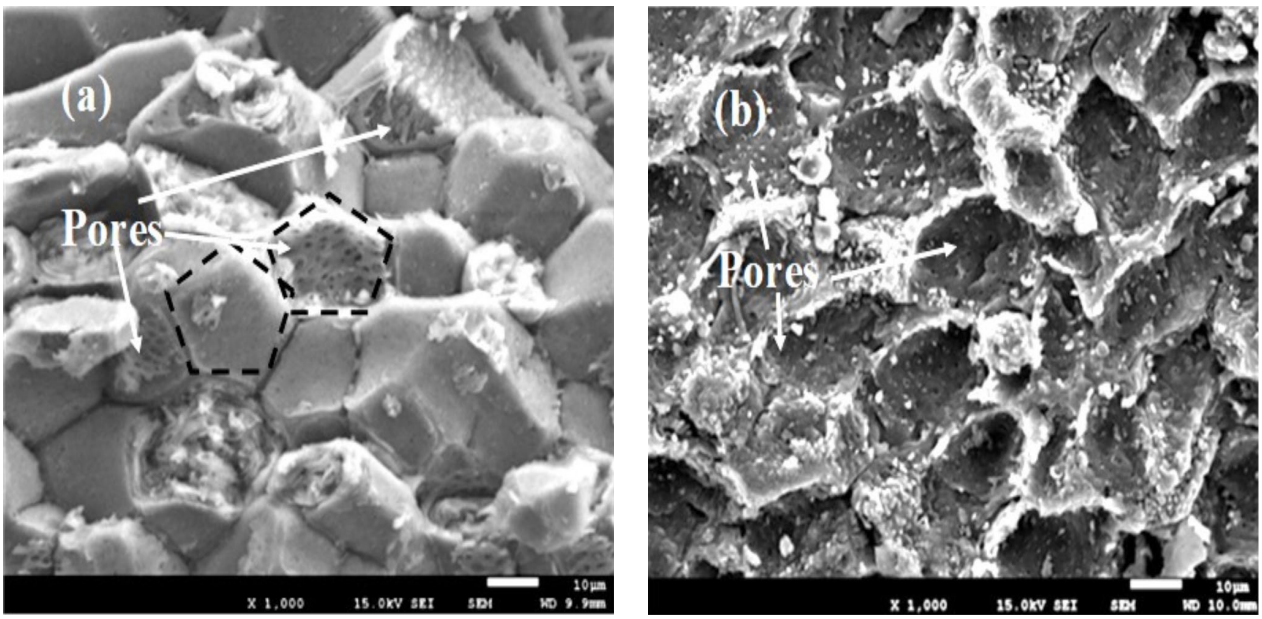

Fig. 2. SEM micrographs of the (a) palm shells and (b) palm char after pyrolysis

area also confirmed that following pyrolysis, more microporous structures had been created (TABLE 4).

TABLE 4

BET surface area measurement of palm shells and palm char after pyrolysis

Samples	BET surface area (m^2/g)	Total pore volume (m^3/g)	Micropore pore volume (m^3/g)	Pore size (nm)
Palm shells	1.8839	5.115×10^{-9}	1.63×10^{-10}	10.86105
Palm char	1.2747	6.25×10^{-10}	7.42×10^{-10}	1.96148

TABLE 4 demonstrates the BET surface area measurements of carbon reductant before and after pyrolysis. According to the table, palm shell had a small surface area (1.8839 m^2/g) and pore volume size (10.86105 nm), however palm char showed a greater pore size (1.96148 nm) after the pyrolysis process. With the evolution of volatile matter, the action of pyrolysis temperature developed more porous structures [13,22]. Cetin et. al. reported that the thermochemical conversion process increased the surface area of the biomass char with high reactivity caused it to react with gas at a faster rate [44]. The pore size of palm char nearly ~2 nm in size due to the thermal conversion process as the porous material became microporous Micropores are important to the char's reactivity, which is crucial for the reduction process. The SEM micrographs show that the findings were consistent (Fig. 2).

3.3. Effect of palm char as renewable carbon reductant on Malaysian ilmenite ores by carbothermal reduction at 1550°C

Further investigation is on the effect of palm char properties as carbon reductant on two differerent Malaysian ilmenite ores by carbothermal reduction at high temperature of 1550°C with an emphasis on the phase changed using XRD analysis. Perak ilmenite contained of the phases iron (Fe), rutile, titanium carbide (TiC), and pseudobrookite (Fe_2TiO_5), is shown in Fig. 3(a). The ilmenite phase still existed due to the incomplete carbothermal reduction at angles 23.80° and 61.55°. To complete the reduction reaction, the reaction time should be prolong up to 60 minutes however, the present study investigated the reaction less than 30 minutes to avoid the reaction developed high amount of TiC phases. The titanium purification procedure would be challenging if more TiC phase [9,45,46]. From the results, TiC appeared at 35.20°, 41.49° and 42.80° due to palm char had sufficient amount of fixed carbon percentage ~75.72 wt.% (TABLE 2) reacted with titanium dioxide thus, TiC was produced at 1550°C as in Eq. (1). Additionally, the porous carbon structures from palm char (TABLE 4 and Fig. 2) also had an impact on the gas adsorption by widening holes and allowing gases to pass through solid phases, which increased the kinetics and speeds of chemical reactions [47].

$$TiO_{2(s)} + 3C_{(s)} \rightarrow TiC_{(s)} + 2CO_{(g)} \quad (1)$$

$$\Delta G° = 512044 - 328.499 \text{ J/mol}$$

The anatase and brooktie TiO_2 phases in Perak ilmenite (Fig. 1(a)) were converted into rutile, iron, and pseudobrookite phases after carbothermal reduction (Fig. 3(a)). The rutile phase of TiO_2 was more stable than anatase and brookite at higher temperatures [27]. Iron phase is expected developed due to high temperature reaction during carbothermal process. The transformation of Perak ilmenite's hematite phase into metallic iron demonstrated that palm char is a more effective as carbon reductant [22]. The pseudobrookite phase as in Eq. (3) existed from the ilmenite ore direct reacted with rutile produced from Eq. (2) is assumed as the second stage of reduction [48].

Eq. (2) represented the initial stage of the carbothermal reduction reaction between carbon from palm char and ilmenite ore.

$$FeTiO_{3(s)} + C_{(s)} \rightarrow Fe_{(s)} + TiO_{2(s)} + CO_{(g)} \quad (2)$$

$$\Delta G° = 395319 + 314.132 \text{ J/mol}$$

$$FeTiO_{3(s)} + TiO_{2(s)} \rightarrow FeTi_2O_{5(s)} \quad (3)$$

$$\Delta G° = -111497 + 138.326 \text{ J/mol}$$

As contrast to Perak ilmenite, Langkawi ilmenite displayed a distinct phase shift after carbothermal reduction with palm char (Fig. 3(b)). The major phase in reduced sample was pseudobrookite (Fe_2TiO_5) detected at 2θ = 18.11°, 25.57°, 36.63°, 25.50° and 48.86°. As shown in Eqs. (4) and (5), this phase was produced by the indirect reaction of ilmenite with carbon monoxide (CO) or hydrogen (H_2) gases, where the oxygen atoms are predominantly removed to increase the amount of TiO_2 [16]. The reduction reactions were further accelerated by the hydrogen content in the palm char (TABLE 2), which also acted as an indirect reducing agent [49].

$$Fe_2TiO_{5(l)} + 3CO_{(g)} \rightarrow 2Fe_{(s)} + TiO_{2(s)} + 3CO_{2(g)} \quad (4)$$

$$\Delta G° = -11781 - 1.170 \text{ J/mol}$$

$$Fe_2TiO_{5(l)} + 3H_{2(g)} \rightarrow 2Fe_{(s)} + TiO_{2(s)} + 3H_2O_{(g)} \quad (5)$$

$$\Delta G° = 71.639 - 81.507 \text{ J/mol}$$

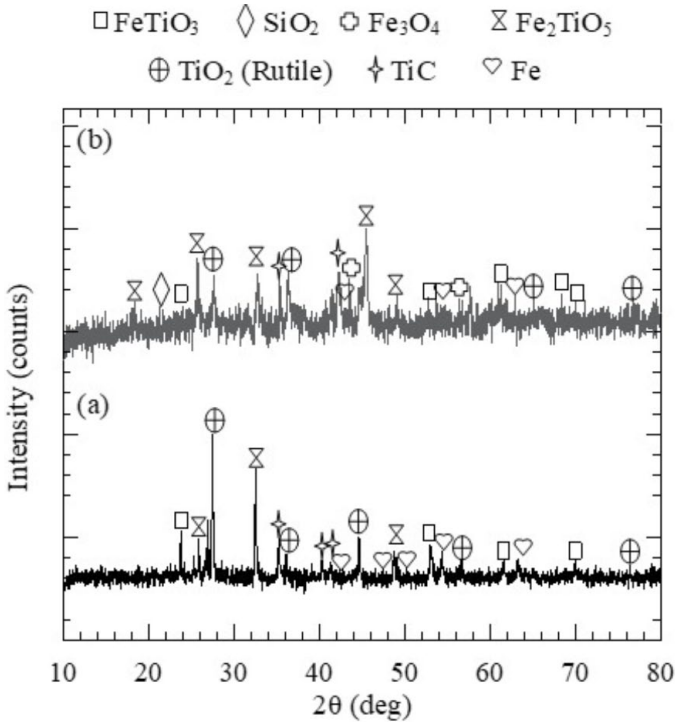

Fig. 3. Phase transformations of Malaysian ilmenite ores using palm char as renewable carbon reductant by carbothermal reduction at 1550°C (a) Perak ilmenite and (b) Langkawi ilmenite

The gas generated (primarily on CO and CO_2), morphology, and elemental analysis using gas analyser, SEM, and XRF, respectively were presented to validate the phase developed after carbothermal reductions between ilmenite and palm char. The CO/CO_2 generated during reduction at 1550°C as a function of time is presented in Fig. 4. At high-temperature reduction when the palm char surface reacted with ilmenite, it promoted endothermic reactions of Boudouard reaction to generate CO, the reduction of ilmenite proceeded thus producing higher CO/CO_2 gases. This is indicated on the rapid reaction between solid carbons with ilmenite and iron oxide for phase conversion into titanium dioxide and iron [22]. The cumulative mol for CO was observed for sample Perak ilmenite/palm char with 4.9112×10^{-5} mol/s and CO_2 with 1.5031×10^{-6} mol/s. Meanwhile, for the sample Langkawi ilmenite/palm char, a slower rate of CO and CO_2 was observed. The relatively low of CO_2 generated was due to the hydrogen content from hydrocarbon may also act as CO_2 gas sink as it produced CO and H_2 [28,48]. From the analysis, the palm char as a renewable carbon reductant was viewed as carbon neutral released the CO_2 neutral [9]. In addition, the carbon and oxygen removed from the gas generation using palm char for reduction of ilmenite ores were increased with time due to the rapid evolution of volatile matter and the mineral matter available [17] such as Fe_2O_3 as in TABLE 2.

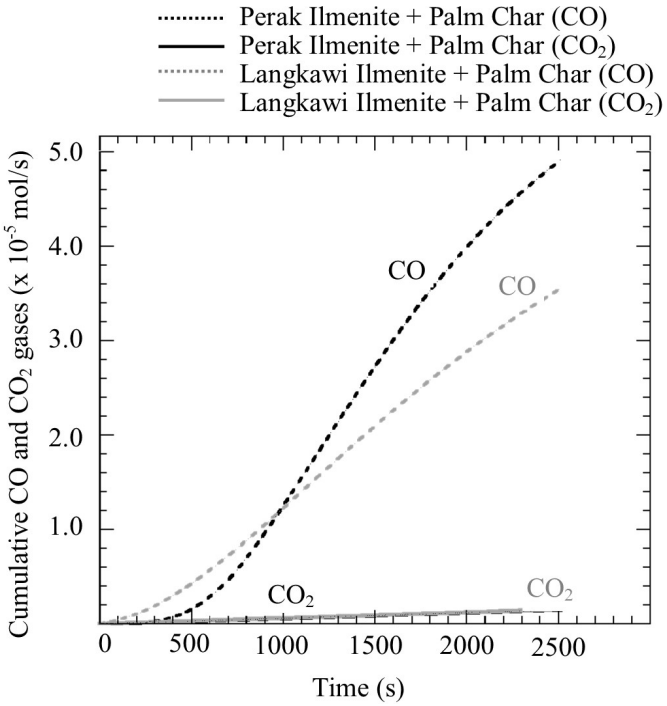

Fig. 4. Cumulative gases generated (CO and CO_2) from gas analyser during carbothermal reduction reaction at 1550°C as function of time for both ilmenite with palm char

Fig. 5(a) and 5(b) demonstrated SEM images after carbothermal reduction with elemental analysis. After the carbothermal reduction of ilmenite ores, the structure had an extremely fine-grained mixed-phase containing rutile, Fe, and reduced ilmenite formed. At 1550°C, ilmenite was reduced into rutile, pseudobrookite and titanium oxides (Fig. 5 and Fig. 3). As can

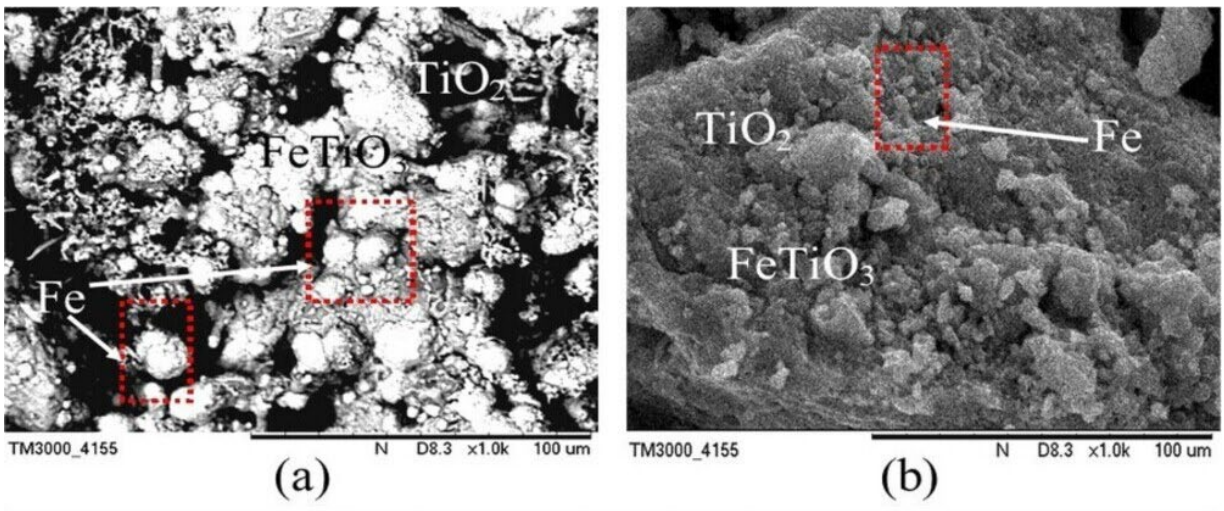

Element (wt.%)	(a) Perak Ilmenite	(b) Langkawi Ilmenite
Fe	18.41	9.28
TiO_2	35.76	22.72

Fig. 5. SEM micrograph of (a) Perak ilmenite with palm char and (b) Langkawi ilmenite with palm char after carbothermal reduction at 1550°C with elemental analysis from XRF

be seen, Perak ilmenite was reduced more TiO_2 (35.76 wt.%) and Fe (18.41 wt.%) when compared to Langkawi (TiO_2 with 22.72 wt.% and Fe with 9.28 wt.%). The tiny spherical/globule structure was detected as an iron phase. It is indicated that the hematite (Fe_2O_3) reduced into iron formation at higher temperatures [1].

In addition, the phase transformation from low-grade-Langkawi ilmenite reacted back with rutile into pseudobrookite is occurred was due to the low amount of TiO_2 in the samples compared to high grade ore (TABLE 1) [18]. From the results, all TiO_2 phases (anatase and brookite) in Langkawi ilmenite transformed into rutile phase comparable to Perak ilmenite, however the quartz phase remained due to high amount of SiO_2 in the sample (TABLE 1 and Fig. 1(b)).

4. Conclusions

Investigations of mineral grade ore and properties of two distinct Malaysian ilmenite ores from different deposit placers, Perak and Langkawi found that Perak ilmenite had confirmed the highest amount of TiO_2 existed as a high-grade ore. The primary phases in the Perak and Langkawi ilmenite were ilmenite, hematite, and TiO_2 of anatase, rutile, and brookite. These phases were converted into pseudobrookite, rutile, TiC, and Fe after carbothermal reduction at 1550°C using palm char . Palm char exhibits as suitable carbon reductant due to the catalytic effects, high fixed carbon content, and volatile matter with porous structure. According to the results, high-grade ilmenite can create more TiO_2 and pure iron, and this will be the basis for investigation for future research.

Acknowledgements

The authors acknowledge the financial support from the Fundamental Research Grant Scheme (FRGS) under Grant Number of FRGS/1/2020/TK0/UNIMAP/02/30 from the Ministry of Higher Education. The authors also acknowledge the support from Research Management and Innovation Center (RMIC), Faculty of Mechanical Engineering Technology and Faculty of Chemical Engineering Technology, Universiti Malaysia Perlis, (UniMAP) for this research.

Conflict of Interest

Authors declare no conflict of interest.

REFERENCES

[1] N.F.M. Yunos, J.H. Chong, A.I. Mohamed, M.A. Idris, Phase Evolution during Carbothermal Reduction of Langkawi Ilmenite Ore at Different Reaction Times. Mater. Sci. For., (2020). DOI: https://doi.org/10.4028/www.scientific.net/MSF.1010.391.

[2] A.I. Mohammed, N.F.M. Yunos, M.A. Idris, Z.A.Z. Jamal, N.F. Hayazi, T. Nomura, Mineralogical Characterizations of Langkawi Ilmenite Ore for Carbothermal Reduction. Int. J. of Nanoelect. Mats. **15** (1) (2022).

[3] A. Yaraghi, M.H.A. Sapri, N. Baharun, S.A. Rezan, N.I. Shoparwe, S. Ramakrishnan, K.S. Ariffin, M.N.A. Fauzi, H. bt. Zabidi, H. Ismail, H.H. Seli, Aeration Leaching of Iron from Nitrided Malaysian Ilmenite Reduced by Polystyrene-Coal Reductant, Procedia Chem. **19** (2016). DOI: https://doi.org/10.1016/j.proche.2016.03.075

[4] E. Ahmadi, A. Fauzi, H. Hussin, N. Baharun, K.S. Ariffin, S.A. Rezan, Synthesis of Titanium Oxycarbonitride by Carbothermal Reduction and Nitridation of Ilmenite with Recycling of Polyethylene Terephthalate (PET). Int. J. Miner. Metall. Mater. **24** (2017).
DOI: https://doi.org/10.1007/s12613-017-1425-2

[5] A.I. Mohammed, N.F.M. Yunos, M.A. Idris, N.H. Najmi, Z. Jamal, T. Nomura. Phase Transformations of Langkawi Ilmenite Ore during Carbothermal Reduction using Palm Char as Renewable Reductant. Chem. Eng. Res. and Design. **178** (2022).
DOI: https://doi.org/10.1016/j.cherd.2021.12.048

[6] C. Perks, G. Mudd, Titanium, Zirconium Resources and Production: A State of the Art Literature Review. Ore Geol. Rev. **107** (2019). DOI: https://doi.org/10.1016/j.oregeorev.2019.02.025

[7] C.S. Kucukkaragoz, R.H. Eric, Solid State Reduction of a Natural Ilmenite. Miner. Eng., (2006).
DOI: https://doi.org/10.1016/j.mineng.2005.09.015

[8] K. Nowinska, Mineralogical and Chemical Characteristics of Slags from the Pyrometallurgical Extraction of Zinc and Lead. Minerals **10** (2020).
DOI: https://doi.org/10.3390/min10040371

[9] R.K. Zinke, W.H. Werkheiser, Critical Mineral Resources of the United States – Economic and Environmental Geology and Prospects for Future Supply: U.S. Geological Survey Professional Paper **1802** (2014), Encycl. Toxicol. Third Ed.

[10] W. Spencer, D. Ibana, P. Singh, A.N. Nikoloski, Effect of Ilmenite Properties on Synthetic Rutile Quality. Miner. Eng. **177** (2022).
DOI: https://doi.org/10.1016/j.mineng.2021.107365

[11] M.A.R. Dewan, G. Zhang, O. Ostrovski, Carbothermal Reduction of Titania in Different Gas Atmospheres. Metall. Mater. Trans. B Process Metall. Mater. Process. Sci. **40** (2009).
DOI: https://doi.org/10.1007/s11663-008-9205-z

[12] A.D. Jara, A. Betemariam, G. Woldetinsae, J.Y. Kim, Purification, Application and Current Market Trend of Natural Graphite: A review. Int. J. Min. Sci. Technol. **29**, 671-689 (2019).
DOI: https://doi.org/10.1016/j.ijmst.2019.04.003

[13] A.A. Adel, N.F.M. Yunos, M.A. Idris, L.I.G. Togang. Investigation on Phase Evaluation of Ilmenite Ore by Carbothermal Reduction and Carboiodination Reaction. Int. J. of Nanoelec. and Mats. **16** (December) (2023).
DOI: https://doi.org/10.58915/ijneam.v16iDECEMBER.415

[14] X. Wang, Z. Lu, L. Jia, F. Li, Preparation and Properties of Low-Cost porous Titanium by using Rice Husk as Hold Space. Prog. Nat. Sci. Mater. Int. **27** (2017).
DOI: https://doi.org/10.1016/j.pnsc.2017.04.014

[15] J.H Kim, J.P. Ao, G. Biyou, Y.T. Biao, Effect of Pyrolysis Conditions on the Physicochemical Properties of Graphitic Carbon Nitride for Visible-Light-Driven Photocatalytic Degradation. Arch. Metall. Mater. **65** (3), 1111-1116 (2020).
DOI: https://doi.org/10.24425/amm.2020.133226

[16] A. Setiawan, M.A. Rhamdhani, M.I. Pownceby, N.A.S. Webster, S. Harjanto, Kinetics and Mechanisms of Carbothermic Reduction of Weathered Ilmenite Using Palm Kernel Shell Biomass, J. Sustain. Metall. **7** (2021).
DOI: https://doi.org/10.1007/s40831-021-00457-w

[17] A.N. Ismail, N.M. Yunos, S.B. Jamaludin, N.H. Najmi, M.A. Idris, Reduction of FeO in EAF steelmaking slag with palm shells under different activation methods. ARPN J. of Eng. and App. Sci. **11** (16) (2016).

[18] N.A. Nasrun, N.F.M. Yunos, M.A. Idris, S.R.R. Munusamy, N. Takahiro, S.A. Rezan, Phase Reduction and Thermodynamic Analysis of Ilmenite Ore by Carbothermal-Iodination using Different Carbon Reductants. Int. J. of Nanoelec. and Mats. **16** (December) (2023).
DOI: https://doi.org/10.58915/ijneam.v16iDECEMBER.409

[19] D. Hu, A. Dolganov, M. Ma, B. Bhattacharya, M.T. Bishop, G.Z. Chen, Development of the Fray-Farthing-Chen Cambridge Process: Towards the Sustainable Production of Titanium and Its Alloys. JOM. **70** (2018).
DOI: https://doi.org/10.1007/s11837-017-2664-4

[20] T. Hu, X. Lv, C. Bai, Z. Lun, G. Qiu, Reduction Behavior of Panzhihua Titanomagnetite Concentrates with Coal. Metall. Mater. Trans. B Process Metall. Mater. Process. Sci. **44**, 252-260 (2013).
DOI: https://doi.org/10.1007/s11663-012-9783-7

[21] N.H. Najmi, N.F.M. Yunos, N.K. Othman, M.A. Idris, The Correlation between Structural and Reduction Kinetics of Carbon from Agricultural Waste with Hematite. J. Mater. Res. Technol. **8** (2019). DOI: https://doi.org/10.1016/j.jmrt.2018.11.014

[22] J. Yu, Y. Li, Y. Lv, Y. Han, P. Gao, Recovery of Iron from High-Iron Red Mud using Suspension Magnetization Roasting and Magnetic Separation. Miner. Eng. **178** (2022).
DOI: https://doi.org/10.1016/j.mineng.2022.107394

[23] Q. Meng, Y. Du, Z. Yuan, Y. Xu, X. Zhao, L. Li, Study on the Mineral Characteristics and Separation Performances of a Low-TiO_2 Ilmenite. Miner. Eng. **179** (2022).
DOI: https://doi.org/10.1016/j.mineng.2022.107458

[24] E. Ahmadi, N.I. Shoparwe, N. Ibrahim, S.A.R. Sheikh Abdul Hamid, N. Baharun, K.S. Ariffin, H. Hussin, M.N. Ahmad Fauzi, The Effects of Experimental Variables on Iron Removal from Nitrided Malaysian Ilmenite by Becher Process, (2018).
DOI: https://doi.org/10.1007/978-3-319-95022-8_113

[25] N. Ibrahim, E. Ahmadi, S.A. Rahman, M.N.A. Fauzi, S.A. Rezan, Extraction of Titanium from Low-/iron Nitrided Malaysian Ilmenite by Chlorination. (2017).
DOI: https://doi.org/10.1063/1.4974426

[26] R. Ren, Z. Yang, L.L. Shaw, Polymorphic Transformation and Powder Characteristics of TiO_2 during High Energy Milling. J. Mater. Sci. **35** (2000).
DOI: https://doi.org/10.1023/A:1026751017284

[27] B. Jagustyn, I. Patyna, A. Skawińska, C. Processing, Evaluation of Physicochemical Properties of Palm Kernel Shell as Agro Biomass used in the Energy Industry, 556-559 (2013).

[28] M. Sommerfeld, B. Friedrich, Replacing Fossil Carbon in the Production of Ferroalloys with a Focus on Bio-Based Carbon: A review. Minerals **11** (2021).
DOI: https://doi.org/10.3390/min11111286

[29] T.Y.A. Fahmy, Y. Fahmy, F. Mobarak, M. El-Sakhawy, R.E. Abou-Zeid, Biomass Pyrolysis: Past, Present, and Future. Environ. Dev. Sustain. **22** (2020).
DOI: https://doi.org/10.1007/s10668-018-0200-5

[30] U. Kumar, S. Maroufi, R. Rajarao, M. Mayyas, I. Mansuri, R.K. Joshi, V. Sahajwalla, Cleaner Production of Iron by using Waste Macadamia Biomass as a Carbon Resource. J. Clean. Prod. **158** (2017).
DOI: https://doi.org/10.1016/j.jclepro.2017.04.115

[31] K. Li, J. Zhang, M. Barati, R. Khanna, Z. Liu, J. Zhong, X. Ning, S. Ren, T. Yang, V. Sahajwalla, Influence of Alkaline (Na, K) Vapors on Carbon and Mineral Behavior in Blast Furnace Cokes. Fuel **145** (2015).
DOI: https://doi.org/10.1016/j.fuel.2014.12.086

[32] H. Mandova, S. Leduc, C. Wang, E. Wetterlund, P. Patrizio, W. Gale, F. Kraxner, Possibilities for CO_2 Emission Reduction using Biomass in European Integrated Steel Plants. Biomass and Bioenerg. **115** (2018).
DOI: https://doi.org/10.1016/j.biombioe.2018.04.021

[33] A. Abdalazeez, T. Li, W. Wang, S. Abuelgasim, A brief review of CO_2 Utilization for Alkali Carbonate Gasification and Biomass/Coal Co-Gasification: Reactivity. Products and Process, J. CO_2 Util. **43** (2021). DOI: https://doi.org/10.1016/j.jcou.2020.101370

[34] A.A. El-Tawil, H.M. Ahmed, L.S. Ökvist, B. Björkman, Self-reduction Behavior of Bio-Coal Containing Iron Ore Composites. Metals (Basel) **10** (2020).
DOI: https://doi.org/10.3390/met10010133

[35] L. Riva, A. Cardarelli, G.J. Andersen, T.V. Buø, M. Barbanera, P. Bartocci, F. Fantozzi, H.K. Nielsen, On the Self-Heating Behavior of Upgraded Biochar Pellets Blended with Pyrolysis Oil: Effects of Process Parameters. Fuel **278** (2020).
DOI: https://doi.org/10.1016/j.fuel.2020.118395

[36] N.F.M. Yunos, M. Zaharia, M.A. Idris, D. Nath, R. Khanna, V. Sahajwalla, Recycling Agricultural Waste from Palm Shells during Electric Arc Furnace Steelmaking. Energ. Fuels (2012).
DOI: https://doi.org/10.1021/ef201184h

[37] H. Suopajärvi, K. Umeki, E. Mousa, A. Hedayati, H. Romar, A. Kemppainen, C. Wang, A. Phounglamcheik, S. Tuomikoski, N. Norberg, A. Andefors, M. Öhman, U. Lassi, T. Fabritius, Use of Biomass in Integrated Steelmaking – Status Quo, Future Needs and Comparison to Other low-CO_2 Steel Production Technologies. Appl. Energy **213** (2018).
DOI: https://doi.org/10.1016/j.apenergy.2018.01.060

[38] P.E. Imoisili, K.O. Ukoba, T. Jen, Synthesis and Characterization of Amorphous Mesoporous Silica from Palm Kernel Shell Ash. Boletín La Soc. Española Cerámica Vidr. **59**, 159-164 (2019).
DOI: https://doi.org/10.1016/j.bsecv.2019.09.006

[39] A.V. Bridgwater, Review of Fast Pyrolysis of Biomass and Product Upgrading. Biomass Bioenerg. **38** (2012).
DOI: https://doi.org/10.1016/j.biombioe.2011.01.048

[40] R. Chatterjee, B. Sajjadi, W.Y. Chen, D.L. Mattern, N. Hammer, V. Raman, A. Dorris, Effect of Pyrolysis Temperature on Physico-Chemical Properties and Acoustic-Based Amination of Biochar for Efficient CO_2 Adsorption. Front. Energy Res. **8** (2020).
DOI: https://doi.org/10.3389/fenrg.2020.00085

[41] K.V. Shah, M.K. Cieplik, C.I. Betrand, W.L. Kamp, H.B. Vuthaluru, Correlating the Effects of Ash Elements and Their Association in the Fuel Matrix with the Ash Release during Pulverized Fuel Combustion. Fuel Process. Technol. **91** (2010).
DOI: https://doi.org/10.1016/j.fuproc.2009.12.016

[42] H.P. Yuchi, C.X. Mo, Z.W. Fu, X.Q. Ma, W.Z. Zhang, K. Wu, Effect of Alkali Metal on Reduction of Iron Oxide by Sectioning Method. J. Iron Steel Res. **30** (2018).
DOI: https://doi.org/10.13228/j.boyuan.issnl001-0963.20180102

[43] E. Cetin, B. Moghtaderi, R. Gupta, T.F. Wall, Influence of Pyrolysis Conditions on the Structure and Gasification Reactivity of Biomass Chars. Fuel **83** (2004).
DOI: https://doi.org/10.1016/j.fuel.2004.05.008

[44] J.G.P. Binner, N.A. Hassine, T.E. Cross, The Possible Role of the Pre-Exponential Factor in Explaining the Increased Reaction Rates Observed during the Microwave Synthesis of Titanium Carbide. J. Mater. Sci. **30** (1995).
DOI: https://doi.org/10.1007/BF00351548

[45] S.K. Gupta, P. Grieveson, Reduction Behavior of Ilmenite with Carbon at 1240°C. Metall. Mater. Trans. B. **26** (1995).
DOI: https://doi.org/10.1007/BF02660983

[46] C. He, C. Zheng, W. Dai, T. Fujita, J. Zhao, S. Ma, X. Li, Y. Wei, J. Yang, Z. Wei, Purification and Phase Evolution Mechanism of Titanium Oxycarbide (Ticxoy) Produced by the Thermal Reduction of Ilmenite. Minerals **11** (2021).
DOI: https://doi.org/10.3390/min11020104

[47] N.J. Welham, A Parametric Study of the Mechanically Activated Carbothermic Reduction of Ilmenite. Miner. Eng. **9** (1996).
DOI: https://doi.org/10.1016/S0892-6875(96)00115-X

[48] N.F.M. Yunos, M.A. Idris, N.A. Nasrun, A.Kurniawan, T. Nomura, S.A. Rezan, Structural Characterizations and Phase Transition on the Reducibility of Ilmenite Ore with Different Carbon Reductants by Carbothermal Reduction Under Hydrogen Atmosphere. J. of Sust. Metall. **9** (2023).
DOI: https://doi.org/10.1007/s40831-023-00760-8